



Northern Hemisphere stratospheric winds in higher midlatitudes: longitudinal distribution and long-term trends

M. Kozubek, P. Krizan, and J. Lastovicka

Institute of Atmospheric Physics ASCR, Bocni II, 14131 Prague, Czech Republic

Correspondence to: M. Kozubek (kom@ufa.cas.cz)

Received: 19 April 2014 – Published in Atmos. Chem. Phys. Discuss.: 20 June 2014

Revised: 4 February 2015 – Accepted: 9 February 2015 – Published: 27 February 2015

Abstract. The Brewer–Dobson circulation (mainly meridional circulation) is very important for stratospheric ozone dynamics and thus for the overall state of the stratosphere. There are some indications that the meridional circulation in the stratosphere could be longitudinally dependent, which would have an impact on the ozone distribution. Therefore, we analyse here the meridional component of the stratospheric wind at northern middle latitudes to study its longitudinal dependence. The analysis is based on the NCEP/NCAR-1 (National Centers for Environmental Prediction and the National Center for Atmospheric Research), MERRA (Modern Era-Retrospective Analysis) and ERA-Interim (European Centre for Medium-Range Weather Forecasts (ECMWF) Re-Analysis Interim) reanalysis data. The well-developed two-core structure of strong but opposite meridional winds, one in each hemisphere at 10 hPa at higher northern middle latitudes, and a less pronounced five-core structure at 100 hPa are identified. In the central areas of the two-core structure the meridional and zonal wind magnitudes are comparable. The two-core structure at 10 hPa is almost identical for all three different reanalysis data sets in spite of the different time periods covered. The two-core structure is not associated with tides. However, the two-core structure at the 10 hPa level is related to the Aleutian pressure high at 10 hPa. Zonal wind, temperature and the ozone mixing ratio at 10 hPa also exhibit the effect of the Aleutian high, which thus affects all parameters of the Northern Hemisphere middle stratosphere. Long-term trends in the meridional wind in the “core” areas are significant at the 99 % level. Trends of meridional winds are negative during the period of ozone depletion development (1970–1995), while they are positive after the ozone trend turnaround (1996–2012). Meridional wind trends are independent of the sudden stratospheric

warming (SSW) occurrence and the quasi-biennial oscillation (QBO) phase. The influence of the 11-year solar cycle on stratospheric winds has been identified only during the west phase of QBO. The well-developed two-core structure in the meridional wind illustrates the limitations of application of the zonal mean concept in studying stratospheric circulation.

1 Introduction

Stratospheric winds play an important role in stratospheric chemistry through the transport of long-lived species, but they could also create transport barriers, which could isolate the polar vortex in winter (Shepherd, 2007, 2008). Simultaneously with the chemical processes, the trace gas distribution modulates the radiative forcing in the stratosphere. The changes in stratospheric wind, namely the strengthening of the westerly polar vortex and its poleward shift, are coupled with ozone depletion and temperature changes (Scaife et al., 2012). For example, the unprecedented ozone loss in the Arctic in 2011 was caused by extreme meteorological conditions (e.g. Pommereau et al., 2013; Manney et al., 2011). The Antarctic ozone hole intensification over the 1980–2001 period is not solely related to the trend in chemical losses but more specifically to the balance between the trends in chemical losses and ozone transport (Monier and Weare, 2011a). One of the most studied circulation structures in the stratosphere is the Brewer–Dobson circulation. A detailed description of this circulation can be found in Butchart (2014). Many model studies reveal an acceleration of the residual mean circulation and the Brewer–Dobson circulation due to the increasing greenhouse gas (GHG) concentration (Oberländer et al., 2013; Lin and Fu, 2013; Oman et al., 2009). How-

ever, the age of air data does not confirm a simple pattern of reduction of the age of air as a consequence of the Brewer–Dobson circulation intensification (Engel et al., 2009; Stiller et al., 2012; Waugh and Hall, 2002). The most recent complex analysis of observational information reveals a reduction of the age of air in the lower stratosphere but an opposite effect in the middle and upper stratosphere (Ray et al., 2014). Monier and Weare (2011b) found some weakening of the northern winter Brewer–Dobson circulation in the polar region in reanalyses ERA-40 (ECMWF Re-analysis for 40 years) and R-2 (NCEP-DOE Reanalysis 2). Some changes in stratospheric wind (strengthening of the westerly polar vortex and its poleward shift, changes in the Brewer–Dobson circulation) are coupled with ozone depletion and also temperature changes. Possible interactions between changes in the stratospheric dynamics and climate changes in the troposphere have been described by Hartmann et al. (2000), Scaife et al. (2012) and Deckert and Dameris (2008). The stratospheric QBO and downward feedback from the stratospheric vortex to tropospheric weather systems have been reported to be relevant both in the context of weather prediction and climate (Baldwin and Dunkerton, 1999; Baldwin et al., 2003; Sigmond et al., 2008; Marshall and Scaife, 2009; Wang and Chen, 2010). Moreover, stratospheric wind (zonal and meridional) affects vertically propagating atmospheric waves, which control the transport circulation in the stratosphere and mesosphere (Holton and Alexander, 2000).

It is generally accepted that the meridional wind component in the stratosphere is much weaker than the zonal wind component. However, as we show later, it is not always the case. Many studies use zonal mean winds for their analyses. The Northern Hemisphere has a pronounced distribution of continents, mountain regions and oceans, which is reflected in the troposphere as well as the stratosphere. Some phenomena introduce longitudinal differences into wind pattern, for example the El Niño–Southern Oscillation – ENSO (e.g. Weare, 2010). The total ozone in the winter higher middle latitudes has a strong longitudinal dependence, with the maximum–minimum difference being more than 100 Dobson Units (DU) (e.g. Mlch, 1994). Bari et al. (2013) found longitudinal dependence of residual winds in the stratosphere and, through impact on the Brewer–Dobson circulation, changes in global circulation, distributions and concentration of stratospheric ozone, and water vapour in the stratosphere and lower mesosphere for 2001–2006. Therefore we study the longitudinal structure of meridional wind (and other parameters) in the stratosphere as a phenomenon of non-zonality, and the long-term evolution of this longitudinal structure, based on the long-term reanalyses' data series. This is the main aim of this paper.

Our study of longitudinal distribution of meridional and zonal wind should reveal whether and where the meridional wind is comparable to the zonal wind. The results could have an impact on BDC circulation in terms of longitudinal distribution, which is very important for ozone transport in

the stratosphere. The distribution of meridional wind, among other things, is very important for wave propagation in the stratosphere (Matsuno, 1970; Kodera et al., 1990).

To test the temporal stability of longitudinal distribution, long-term trends at latitudes of the most pronounced longitudinal structures are calculated. Ozone concentration in the northern middle latitudes changed its trend (from negative to positive) in the mid-1990s (e.g. Harris et al., 2008). Since ozone is the main contributor to heating of the stratosphere via absorption of solar radiation, this turnaround of ozone trend also influences the behaviour of other stratospheric parameters (changes in temperature and wind trends), and it even affects the mesosphere and lower thermosphere (e.g. Lastovicka et al., 2012). Since ozone trends in the northern middle latitudes changed in the mid-1990s (e.g. Harris et al., 2008), trends in stratospheric dynamics are expected to be altered by the ozone recovery and thus trends in the periods before and after the mid-1990s are examined separately.

Sudden stratospheric warming (SSW) and the quasi-biennial oscillation (QBO) are known to have an important impact on the stratosphere, including its circulation (Limpasuvan et al., 2004; Naito and Hirota, 1997; Labitzke and van Loon, 1988). The stratosphere is also influenced by solar activity (e.g. Gray et al., 2010, and references herein). The impact of these phenomena on stratospheric circulation, particularly on the observed longitudinal structures in meridional wind, deserves attention and analysis.

This paper focuses on two topics:

1. Longitudinal distribution of the meridional wind component at different pressure levels and the possible reasons for its behaviour. Therefore the longitudinal distributions of geopotential height and zonal wind component will also be calculated. This will be accompanied by trend analysis of observed longitudinal structures. The results of the meridional wind distribution analysis are described in Sect. 3.1. Long-term trends in the longitudinal distribution of meridional wind are also examined, and the results are presented in Sect. 3.2.
2. Trend analysis of stratospheric total horizontal wind and meridional component with connection to QBO, SSW (mainly wave-driven) and solar activity. The results are described in Sect. 3.3.

The structure of the paper is as follows. In Sect. 2, the data and methods are described. Then, in Sect. 3, the results of analysis are shown and, in Sect. 4, they are briefly discussed. Section 5 provides conclusions.

2 Data and methods

Stratospheric winds have been measured from the ground using active and passive techniques (Hildebrand et al., 2012; Rüfenacht et al., 2012). From space they were measured by

the High Resolution Doppler Imager (HRDI) on the Upper Atmospheric Research Satellite (UARS) covering 10–35 km and 60° S–60° N, using the molecular oxygen A and B bands (Ortland et al., 1996). Baron et al. (2013) derived winds from SMILES (Superconducting Submillimeter-Wave Limb-Emission Sounder). However, direct wind measurements from satellite do not provide sufficiently long and homogeneous global data series.

Therefore, when studying longitudinal distribution of meridional or zonal wind, we use three independent reanalyses data sets, namely NCEP/NCAR-1 reanalysis (National Centers for Environmental Prediction and the National Center for Atmospheric Research, hereinafter NCEP/NCAR), MERRA (Modern Era-Retrospective Re-Analysis) and ERA-Interim (European Centre for Medium-Range Weather Forecasts (ECMWF) Re-Analysis Interim). The NCEP/NCAR reanalysis is described in detail in Kistler et al. (2001). This reanalysis provides data from 1948 onwards (but the data are more reliable from 1957 onwards, when the first upper-air observations were established) and better global data from 1979 onwards, due to the start of satellite data assimilation. Data are available on the $2.5 \times 2.5^\circ$ grid at specific times: 00:00, 06:00, 12:00 and 18:00 UTC. Vertical resolution is 28 levels from 1000 hPa to the top of the model at 2.7 hPa. The NCEP/NCAR reanalysis system assimilates upper-air observations, but it is only marginally influenced by surface observations because model orography differs from reality (Kistler et al., 2001). ERA-Interim is described by Dee et al. (2011). Data are available from 1979 on the $0.75 \times 0.75^\circ$ grid at 00:00, 06:00, 12:00 and 18:00 UTC. Vertical resolution is 60 levels from 1000 hPa to the top of the model at 1 hPa. The MERRA reanalysis is described in and downloaded from <http://disc.sci.gsfc.nasa.gov>. Data are available from 1979 on the $1.25 \times 1.25^\circ$ grid at 00:00, 06:00, 12:00 and 18:00 UTC. Vertical resolution is 42 levels from 1000 hPa to the top of the model at 0.1 hPa.

According to Kozubek et al. (2014), stratospheric winds from the NCEP/NCAR reanalysis are better for long-term trend analysis than those from ERA-40 and ERA-Interim reanalyses – if we take into account the length of the available period. Neither ERA-40, nor ERA-Interim, nor MERRA separately cover the whole period 1958–2012. On the other hand, the general pattern and long-term changes in stratospheric winds in NCEP/NCAR, ERA-40 and ERA-Interim reanalyses (except for the last 4 years of ERA-40) have not differed in main features from each other since about 1970 (Kozubek et al., 2014); therefore it is possible to use only one of these three reanalyses for trend analysis. The 10.7 cm solar radio flux (from <http://www.esrl.noaa.gov/psd/data/correlation/solar.data>) is used for the solar cycle influence analysis (solar maximum and solar minimum). The QBO data at 50 hPa are taken from <http://www.geo.fu-berlin.de/en/met/ag/strat/produkte/qbo/> and SSW data

are taken from <http://www.geo.fu-berlin.de/en/met/ag/strat/produkte/northpole/index.html>.

For the investigation of longitudinal distribution of meridional wind (two-core structure – Sect. 3.1), zonal wind or geopotential height, we have computed averages throughout the period 1970–2012 for every grid point from 20 to 60° N and for every month. Analysis of the wind speed distribution at 100 hPa (where we can identify influence of the troposphere and study dynamics near the tropopause) and 10 hPa (which is a representative level for the middle stratosphere and determination of major stratospheric warming) at 00:00 UTC or the meridional wind speed distribution at 00:00, 06:00 and 12:00 UTC (for examining possible influence of diurnal and semidiurnal tides) has been done for all three reanalyses.

The trend analysis is focused on middle latitudes (50–60° N), at the pressure level of 10 hPa, in order to investigate the behaviour of wind in the two-core structure area. We also analyse the connection between QBO, SSW and solar activity versus dynamics (stratospheric wind) at 10 hPa. In trend analyses we have used either total horizontal wind or v (meridional) components separately. The total horizontal wind speed is calculated from gridded u (zonal) and v (meridional) components.

The selected latitudes are separated for trend analysis into four sectors (100–160° E – poleward wind core; 160° E–140° W – the sector of the Aleutian height; 140–80° W – equatorward wind core; and 80° W–100° E – the sector not affected by the two-core structure; see Fig. 1 and Sect. 3.1).

We look for trends or differences between different groups in each sector at 10 hPa. The statistical significance threshold of trends has been set at the 95 % level, which is the standard significance level for analyses in meteorology (wind, temperature, etc.), and in some trend analysis it is also set at the 99 % level. We divide data of the whole period into several groups according to QBO (east or west QBO phase) or solar cycle influence (solar maximum years and solar minimum years) and for the trend analysis we divided data into two periods (1970–1995, with decreasing ozone, and 1995–2012, with increasing ozone). We compute trends separately for all these groups with a significance threshold of 95 or 99 %.

3 Results

3.1 Longitudinal distribution of stratospheric meridional winds

The whole-period averages of meridional wind component for each grid point from 60 to 20° N for January at 10 hPa have been computed. These computations have been done for all three reanalyses (MERRA for period 1979–2012, ERA-Interim for 1979–2012 and NCEP/NCAR for 1958–2012). The results are shown in Fig. 1. The top panel shows results for NCEP/NCAR, the middle panel for ERA-Interim and the

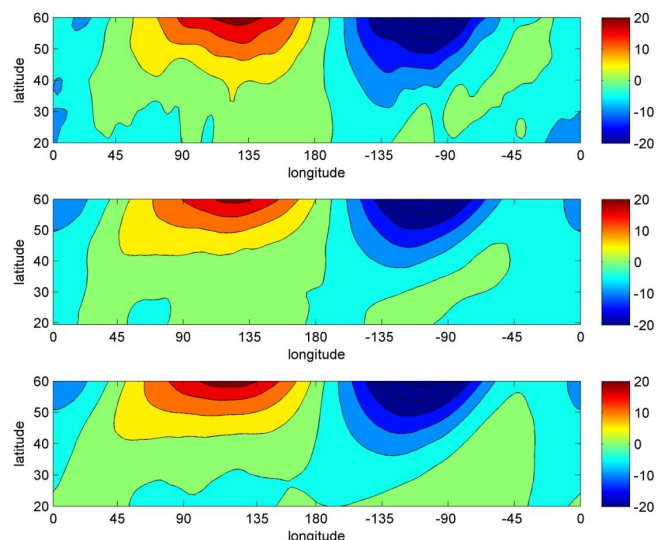


Figure 1. Plot of average meridional wind speed (m s^{-1}) component for January at $20\text{--}60^\circ\text{ N}$, $180^\circ\text{ E--}180^\circ\text{ W}$ and 10 hPa. Top panel NCEP/NCAR (1958–2012), middle ERA-Interim (1979–2012), and bottom MERRA (1979–2012). Positive values (poleward wind): red; negative values (equatorward wind): blue.

bottom panel for MERRA reanalysis. The behaviour of different reanalyses is quite similar in major features despite the different length of time intervals. Figure 1 reveals, at 10 hPa for January, a core of strong poleward wind on the eastern hemisphere at the middle and higher latitudes. This poleward wind changes into equatorward wind core on the western hemisphere at 10 hPa (at similar amplitude to the eastern hemisphere). Both the poleward and equatorward peaks (centres of the cores in Fig. 1) are statistically significant at the 99 % level for NCEP/NCAR reanalysis. The results of similar analysis for 100 hPa are shown in Fig. 2. Generally, winds are stronger at 10 hPa (up to 20 m s^{-1}) than at 100 hPa (up to 10 m s^{-1}). At 100 hPa there is a five-core structure, which is much less pronounced than the two-core structure at 10 hPa. The same analysis as in Fig. 1 is shown in Fig. 3 for July at 10 hPa. Figure 3 reveals no two-core structure at 10 hPa for summer – it occurs only in winter. Winds in July are weaker than in January, and the distribution has no regular structure compared with January. We have done the same analysis for the higher pressure level of 5 hPa (not shown), and the differences between the eastern and western hemispheres (two-core structure) have been found to grow with increasing height.

Figure 4 shows a climatology based on the NCEP/NCAR reanalysis over the period 1958–2012 for January at 10 hPa pressure level for data from 00:00 (top panel), 06:00 (middle panel) and 12:00 UTC (bottom panel). There are almost no differences in the main features. Therefore, we can conclude that the two-core structure with opposite meridional winds is not caused by diurnal or semidiurnal tides. The other pos-

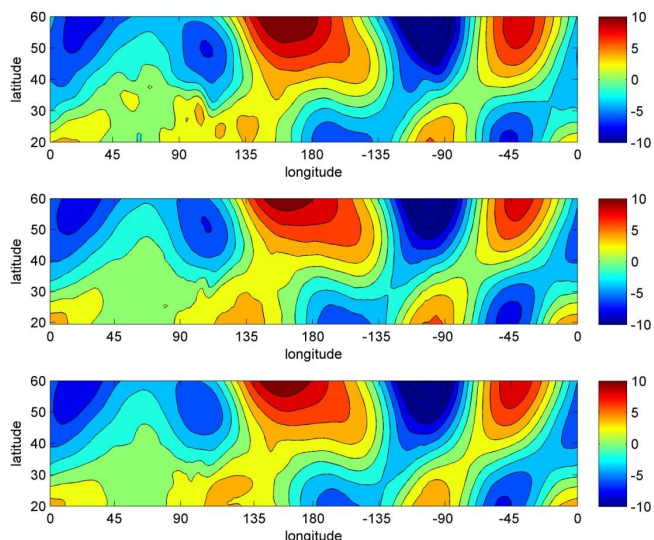


Figure 2. The same as Fig. 1 but for 100 hPa.

sibility for this structure could be dynamical reasons, which are discussed in the next paragraph.

The wind field is closely associated with the distribution of geopotential height because of dynamical reasons (principle of mass conservation, hydrostatic equation, etc.). Figure 5 shows a distribution of geopotential height at 10 hPa – again for all three reanalyses. The Aleutian pressure high centred at about $40\text{--}55^\circ\text{ N}$, 180° E is well developed at 10 hPa. This Aleutian high can block the zonal winter eastward winds. This should result in poleward meridional flow at the front (western) side and an equatorward meridional flow at the back (eastern) side as a consequence of the flow along the strong anticyclone. Such a flow coincides with the observed two-core structure at 10 hPa with the poleward meridional component of wind on the eastern hemisphere and the equatorward meridional component on the western hemisphere. The behaviour of zonal wind at 10 hPa, shown in Fig. 6 for all three reanalyses, reveals substantial weakening of zonal wind in and around the region of the Aleutian pressure height; together with strengthening of the meridional component, it results in non-zonal, oblique wind flow. In some locations, like 60° N , 135° E , both wind components are approximately equal. The summertime distribution of geopotential heights at 10 hPa does not display any well-pronounced structure, and therefore no pronounced structure is developed in meridional wind (Fig. 3). The distribution of geopotential height resembles the five-core structure in winds in Fig. 2 at 100 hPa on the western hemisphere but not on the eastern one. But, again, this structure is much less pronounced than that at 10 hPa (not shown).

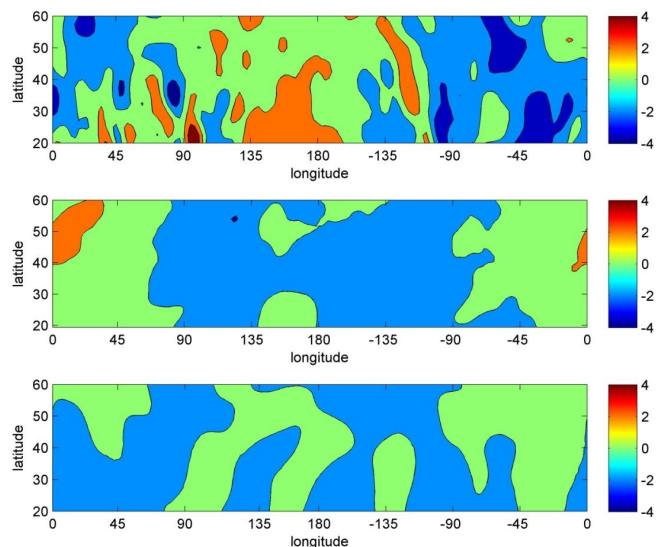


Figure 3. The same as Fig. 1 but for July. Positive values (poleward wind): red; negative values (equatorward wind): blue.

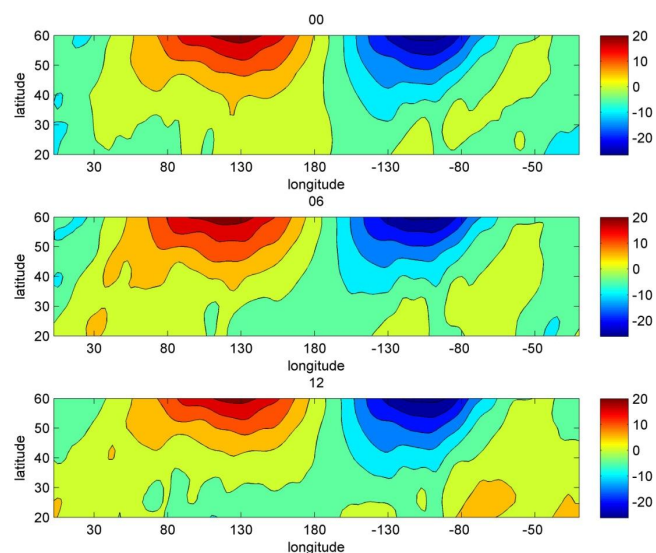


Figure 4. Plot of average meridional wind speed (m s^{-1}) component at 10 hPa for January 1958–2012 at 20–60° N, 180° E–180° W. Top panel: 00:00 UTC; middle: 06:00 UTC; bottom: 12:00 UTC. Positive values (poleward wind): red; negative values (equatorward wind): blue. NCEP/NCAR reanalysis only.

3.2 Trends in meridional wind cores

This analysis is focused on latitudes where the two-core structure at 10 hPa was identified (50–60° N). It is based on the NCEP/NCAR reanalysis only. The trends in meridional wind are shown in Table 1. We can identify change of trends in all four sectors from a positive trend (core strengthening) for period 1970–1995 to a negative trend (core weakening) for 1996–2012. The trends in core sectors (100–160° E and

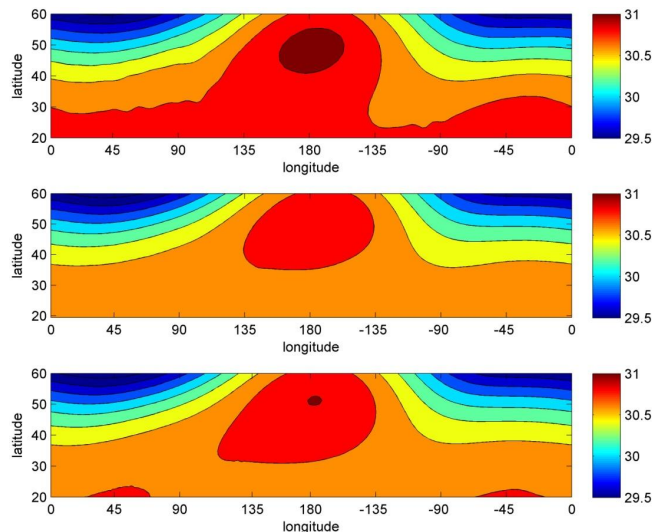


Figure 5. Plot of average geopotential height (km) for January 1958–2012 at 20–60° N, 180° E–180° W. Top panel: NCEP/NCAR (1958–2012); middle: ERA-Interim (1979–2012); bottom: MERRA (1979–2012).

140–80° W) are significant at the 99 % level for 1995–2012, and predominantly at the 95 % level for 1970–2012. Trends in the other two sectors are much smaller and statistically insignificant. The turnaround of trends in total column ozone in the northern middle latitudes in the mid-1990s (e.g. Harris et al., 2008) has an impact on the meridional wind cores – trends in cores also alter; they change from positive before the ozone trend turnaround to negative after. We are not going to speculate as to what extent this turnaround of meridional wind trends is caused by dynamical factors, which is the main cause of the ozone trend turnaround. However, the impact of some external factors on trends in wind is investigated in the next section.

3.3 Impact of solar cycle, SSW and QBO on trends in wind

Further analysis (NCEP/NCAR reanalysis only, we can use a longer period: 1970–2012), which has been done, is comparison between years in the solar cycle maximum and minimum in different QBO phases and trends in different dynamical processes (SSW or no SSW years, east or west QBO years). This analysis is also focused on latitudes where the two-core structure at 10 hPa was identified (50–60° N). It should reveal potential connections between solar cycle, stratospheric dynamics (wind speed) and wave-activity-driven SSW, all under the potential influence of QBO. Stratospheric dynamics and chemistry is influenced by changes in ozone concentration (see e.g. Table 1), so we separately analyse wind in the periods 1970–1995 (with decreasing ozone) and 1995–2012 (with increasing ozone.) Trends are shown for different groups (with and without major SSW years and east or west

Table 1. Winter (December–February) trends (m s^{-1} per year) of meridional wind speed for two periods (1970–1995 and 1996–2012). Pressure level 10 hPa. 70–95 means 1970–1995 and 95–12 means 1995–2012. Trends significant at the 99 % level are highlighted in bold; trends significant at the 95 % level are in italics. Sectors 100–160° E and 140–80° W are the sectors with cores in meridional wind.

10 hPa												
Latitude	50° N				55° N				60° N			
Sector	100 –160° E	160° E –140° W	140 –80° W	80° W –100° E	100 –160° E	160° E –140° W	140 –80° W	80° W –100° E	100 –160° E	160° E –140° W	140 –80° W	80° W –100° E
70–95	0.42	0.10	<i>0.39</i>	0.07	0.48	0.11	<i>0.42</i>	0.03	<i>0.47</i>	0.09	<i>0.42</i>	0.04
95–12	–0.71	–0.15	–0.68	–0.09	–0.68	–0.19	–0.74	–0.06	–0.74	–0.12	–0.67	–0.10

Table 2. Winter (December–February) trends (m s^{-1} per year) of the meridional wind speed for two periods (1970–1995 and 1996–2012). Major SSW: only years when the major SSWs (according to WMO definition) occur; no SSW: years when no major SSW occurs; east QBO: only years under the east phase of QBO; west QBO: only years under the west phase of QBO. Pressure level 10 hPa. 70–95 means 1970–1995 and 95–12 means 1995–2012. Trends significant at the 99 % level are highlighted in bold; trends significant at the 95 % level are in italics.

10 hPa													
Latitude	50° N				55° N				60° N				
Sector	100 –160° E	160° E –140° W	140 –80° W	80° W –100° E	100 –160° E	160° E –140° W	140 –80° W	80° W –100° E	100 –160° E	160° E –140° W	140 –80° W	80° W –100° E	
70–95	0.52	<i>0.21</i>	<i>0.49</i>	0.15	0.57	0.15	0.54	0.12	0.6	0.11	0.55	0.1	major
95–12	–0.61	–0.19	–0.63	–0.1	–0.61	<i>–0.27</i>	–0.67	<i>–0.24</i>	–0.64	–0.22	–0.59	<i>–0.26</i>	SSW
70–95	0.39	<i>0.23</i>	0.46	<i>0.2</i>	0.43	0.19	0.51	0.15	0.49	0.16	0.56	<i>0.18</i>	no
95–12	–0.71	–0.08	–0.42	–0.05	–0.6	–0.11	–0.49	–0.08	–0.64	–0.13	–0.56	–0.1	SSW
70–95	0.37	0.14	0.35	0.09	<i>0.39</i>	<i>0.17</i>	0.42	<i>0.19</i>	0.43	0.19	0.48	0.23	east
95–12	–0.44	<i>–0.24</i>	–0.4	<i>–0.19</i>	–0.48	–0.16	–0.46	–0.11	–0.53	–0.12	–0.51	–0.09	QBO
70–95	0.34	<i>0.19</i>	0.49	<i>0.2</i>	0.41	<i>0.24</i>	0.55	0.21	0.39	<i>0.25</i>	0.59	<i>0.27</i>	west
95–12	–0.5	–0.08	–0.64	–0.04	–0.54	–0.12	–0.62	–0.09	–0.57	–0.17	–0.68	–0.12	QBO

QBO phase years) for December–January–February (DJF), as the strongest two-core structure occurs in January. We analyse the total horizontal wind as well as the meridional component separately to find out which component is more affected by different drivers. The trends for meridional wind are shown in Table 2. We can identify a turnaround of the trends in all four sectors for all four groups (a positive one for period 1970–1995, and a negative one for 1996–2012). There is little, if any, systematic difference in trends between years with and without SSWs; the significant trends are perhaps a little bit stronger in the years with SSWs. Similar conclusions can be drawn for the impact of QBO; there is little dependence of trends on QBO, with perhaps slightly stronger trends for the west phase of QBO.

The trends are significant at the 99 % level (in a few cases only at the 95 % level) in the two sectors where the core structure occurs (100–160° E and 140–80° W). There are only a few significant trends (95 % level) in the other two sectors. There are generally stronger negative significant trends (99 % level) in Table 1 than in Table 2 during the second period (1996–2012) in the core-containing sectors.

The results on the connection of solar cycle and QBO with the total horizontal wind speed are shown in the top panel of

Table 3. At 10 hPa we can observe a positive difference (of 2–5 m s^{-1}) between solar minimum and maximum for the west QBO in both sectors where cores occur. The differences are significant at the 95 % level. The differences are smaller and insignificant in the other two wind sectors. The east QBO does not reveal a systematic or significant difference. Moreover, wind during solar maximum is sometimes stronger than during solar minimum. The differences between the QBO east and QBO west phase are negative during solar minimum (up to 3 m s^{-1}) in all studied sectors. These differences are, again, mainly significant in the two core sectors. Differences between the QBO east and QBO west phase during solar maximum are mainly positive but insignificant.

The bottom panels show the same analysis as the top ones but for the v (meridional) wind component. The differences are smaller than for the total horizontal wind. We cannot find any specific features for all four groups. We can see only a few significant values in different sectors.

The analysis was also done for each month separately, and the largest differences were found in December and January. These results show that solar activity influences the total horizontal wind (i.e. mainly zonal wind) mostly in higher parts

Table 3. Winter (December–February) differences of wind speed (m s^{-1}) for different latitudes and sectors during the whole period. Top panels show the total horizontal wind speed for 10 hPa; bottom panels show the v (meridional) wind component for 10 hPa. Min/east: years under solar minimum and the east phase of QBO conditions; min/west: years under solar minimum and the west phase of QBO; max/east: years under solar maximum and the east phase of QBO conditions; max/west: years under solar maximum and the west phase of QBO. Significant differences at the 95 % level are highlighted in bold.

	50° N				55° N				60° N				Latitude Sector	
	100 –160° E	160° E –140° W	140 –80° W	80° W –100° E	100 –160° E	160° E –140° W	140 –80° W	80° W –100° E	100 –160° E	160° E –140° W	140 –80° W	80° W –100° E		
(min/east)	–1.07	–0.08	–1.47	–0.03	–1.89	–0.28	–1.73	–0.23	–2.77	–0.57	–2.05	–0.53	10 hPa	
–(min/west)														
(max/east)	0.33	–0.27	1.26	–0.46	0.66	–0.42	1.17	–0.44	1.04	–0.18	0.76	–0.27		
–(max/west)														
(min/west)	2.02	0.38	1.39	0.51	2.76	0.81	1.84	0.72	3.19	1.08	2.23	1.01		
–(max/west)														
(min/east)	0.62	0.96	–1.36	1.02	–0.39	0.75	–1.19	0.81	–0.71	0.64	–0.92	0.56		
–(max/east)														
(min/east)	–0.01	0.34	–0.63	0.60	–0.11	–0.29	–0.73	0.79	–0.26	1.14	–0.84	1.12		10 hPa v
–(min/west)														
(max/east)	–0.38	0.2	0.15	0.09	–0.40	–0.52	0.14	0.10	–0.43	0.18	0.17	0.14		
–(max/west)														
(min/west)	–0.17	0.42	1.17	–0.73	–0.20	–0.17	1.39	–0.86	–0.18	–0.95	1.57	–0.99		
–(max/east)														
(min/east)	0.19	–0.29	0.39	–0.22	0.09	–0.11	0.49	–0.17	–0.01	–0.17	0.57	–0.11		
–(max/east)														

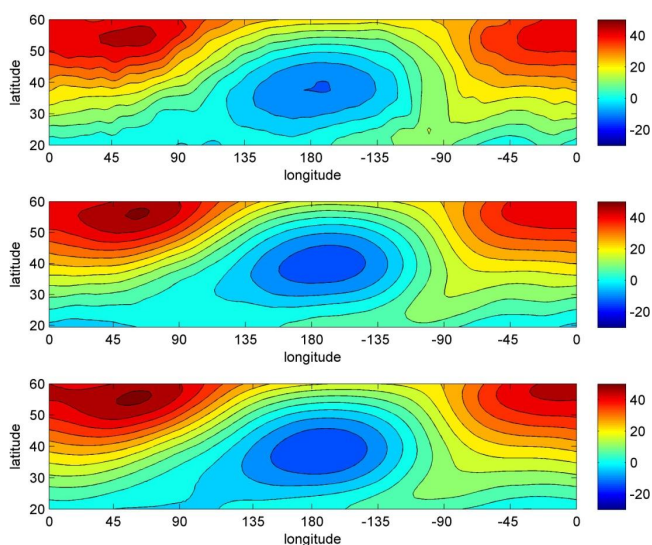


Figure 6. Plot of average zonal wind speed (m s^{-1}) component for January at 20–60° N, 180° E–180° W and 10 hPa. Top panel: NCEP/NCAR (1958–2012); middle: ERA-Interim (1979–2012); bottom: MERRA (1979–2012). Positive values (eastward wind): red; negative values (westward wind): blue.

of the stratosphere (10 hPa) and predominately in the two core sectors (not shown in the paper).

4 Discussion

The results on longitudinal distribution of the meridional and zonal components of stratospheric wind show that the meridional wind forms a well-pronounced two-core structure at 10 hPa in winter. This two-core structure is revealed by NCEP/NCAR, ERA-Interim and MERRA reanalyses in a very similar form, despite the different time periods used (Fig. 1). The wintertime longitudinal distribution at 10 hPa cannot be explained by either diurnal or semidiurnal tides, because there are no differences between the longitudinal distributions of meridional winds at 00:00, 06:00 and 12:00 UTC (Fig. 4). However, the geopotential height analysis reveals the reason for this longitudinal distribution. The well-developed large Aleutian high at 10 hPa (Fig. 5) can block the zonal flow (see Fig. 6), and it pushes the winter eastward winds to the pole (poleward) on the western side of the Aleutian pressure high and back (equatorward) on its eastern side. A comparison of Figs. 1 and 6 shows that the zonal component of stratospheric wind is almost equal to the meridional component in some areas in the cores. This phenomenon could result in wave propagation changes in this part of the stratosphere (at 10 hPa; e.g. Matsuno, 1970; Kodera et al., 1990) and could affect other wave-driven phenomena like SSW. The results show that the deep (upper) branch of the Brewer–Dobson circulation is affected by the longitudinal distribution of meridional wind, which can affect the distribution of total ozone and of age of air in the middle stratosphere.

Therefore, Fig. 7 shows longitudinal distribution of ozone, as well as temperature, at 10 hPa in the middle latitudes

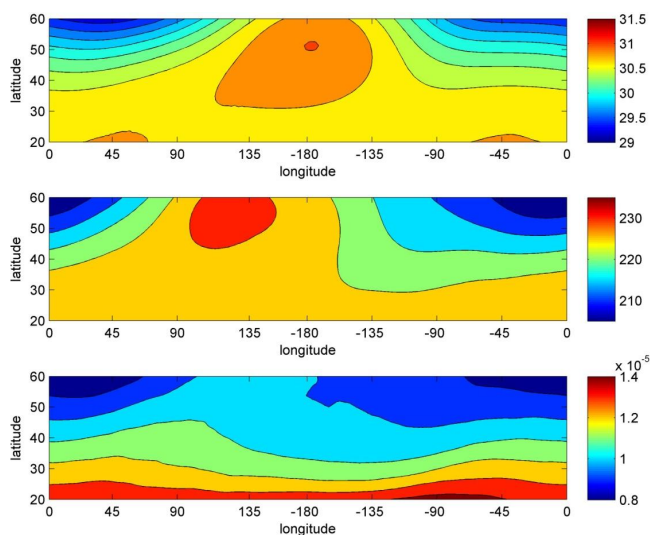


Figure 7. Plot of average geopotential height (km, top panel), temperature (K, middle panel) and ozone mixing ratio (ppmv, bottom panel) for January at 20–60° N, 180° E–180° W and 10 hPa.

(20–60° N). This distribution is consistent with the two-core structure of meridional wind – in the eastern hemisphere, where the intensified poleward meridional wind transports warmer air and more ozone towards higher latitudes (60° N), the temperature and to a lesser extent ozone concentration are increasing; in the western hemisphere core the opposite meridional transport reduces temperature and ozone at higher middle latitudes. Thus all studied parameters – meridional wind, geopotential height, zonal wind, temperature and ozone – agree regarding the main features of the longitudinal variation and provide an internally consistent pattern of the longitudinal variation in the winter middle stratosphere (at 10 hPa) characterized by the two cores of strong meridional wind. This result illustrates limitations of the applicability of the zonal mean approach.

In future studies, processes of the lower and higher levels of the atmosphere (below 100 hPa and above 5 hPa) have to be analysed to find the main driver of these changes in meridional wind direction. To our best knowledge, the longitudinal structure of middle stratosphere circulation at middle latitudes has only been studied by Bari et al. (2013), who simulated a longitudinal structure of residual winds for January 2001–2006 with the HAMMONIA model. Our results agree with this study. They found impact from that longitudinal structure on the Brewer–Dobson circulation and distribution of stratospheric ozone and water vapour (changes in maximum and minimum of O_3 and H_2O and their distributions, their Figs. 7 and 8). Investigation of the longitudinal dependence of stratospheric zonal winds during SSW events with the model HAMMONIA (Miller et al., 2013, their Fig. 6) demonstrates the very longitudinally asymmetric mean state of winter stratospheric zonal winds in HAMMO-

NIA. Moreover, the winds do not only evolve differently during the SSWs; the wind speeds were found to differ by more than 20 m s^{-1} between the four locations at stratospheric altitudes between 100 and 1 hPa.

We identify statistically significant trends in meridional wind (mostly at the 99 % level) in both core sectors at 10 hPa (Table 1). These trends are positive (strengthening of meridional wind) in 1970–1995 (decreasing ozone content) and negative (weakening of meridional wind) in 1996–2012 (increasing ozone content) for both cores. The strengthening of meridional wind in 1970–1995 (Table 1) and opposite trends/tendencies in 1996–2012 is consistent with some strengthening/weakening of the blocking Aleutian pressure high. This is confirmed by trends in the central part of the blocking Aleutian pressure high: $+34.6 \text{ m yr}^{-1}$ for 1970–1995 and -38.3 m yr^{-1} for 1996–2012, both being significant at the 95 % level. The trends are mostly insignificant in the other two sectors (sector not affected by the two-core structure; 160° E–140° W, 80° W–100° E). Reversal of trends in the mid-1990s occurred in both meridional wind and ozone. However, ozone serves here as an indicator rather than a cause of the trend change. Statistical and modelling studies carried out as part of the European FP5 project CANDIDOZ show that the main cause of this change in ozone trends results from changed dynamical behaviour such as EP flux, tropopause height and NAO index trends (Harris et al., 2008). This conclusion is supported by behaviour of the ozone laminae (Lastovicka et al., 2014).

The above results are the reason why we investigate, in Sect. 3.3, the potential effect of some dynamical factors (SSW and QBO), which could be behind the change of trends of both ozone and wind. The change of the meridional wind trend (from positive to negative in the mid-1990s) occurs independently of SSW or QBO (Table 2). We can connect this with changes in ozone trends. The trends in core structure areas are significant (mainly at 99 % level) for all four SSW–QBO combinations (Table 2) as well as for all years trend (trend including all seasons, Table 1). In areas not containing the core structure, more significant trends (95 % level) occur for years with SSWs than without major SSWs. This result could indicate that the unusual conditions in the stratosphere during an SSW can affect meridional wind trends (Brewer–Dobson circulation and ozone transport) even in areas where meridional wind is weak.

According to Shindell et al. (1999) the changes in the upper stratospheric wind are caused partly by changes in the solar irradiance. The impact of the 11-year solar cycle, sometimes in combination with the QBO, on the stratosphere has been described in many papers (e.g. Salby and Callahan, 2000; Labitzke and Kunze, 2009; Limpasuvan et al., 2004; Naito and Hirota, 1997; Labitzke and van Loon, 1988). The influence of solar activity on the total horizontal wind as well as the meridional component is shown in Table 3. Our results agree with the results of other authors (mentioned above), but we specify dependence of solar effect on longitude. The

most statistically significant differences in the total horizontal wind can again be found in the two core sectors. The differences are larger at higher latitudes. This result agrees with previous studies (Labitzke and Kunze, 2009; Labitzke and van Loon, 1988) in which higher latitudes are more affected by changes in solar activity. The analysis of the meridional component does not show any specific features, so we can conclude that solar activity mainly affects the total horizontal wind and its zonal component.

5 Conclusions

Based on data from NCEP/NCAR, ERA-Interim and MERRA reanalyses, the longitudinal distribution of the meridional component of stratospheric wind in winter (January) has been examined for 20–60° N. It reveals a well-pronounced longitudinal distribution of meridional wind at latitudes above 45° N with two cores of strong but opposite meridional winds, one in each hemisphere (eastern and western) at 10 hPa, and a much less pronounced five-core structure at 100 hPa. All three reanalyses provide the same pattern. In summer, such a well-pronounced core structure is absent. The two-core structure at 10 hPa is not caused by tides, as no differences exist between 00:00, 06:00 and 12:00 UTC results. We have identified the strong and well-developed large Aleutian pressure high at 10 hPa, which is capable of explaining qualitatively the two-core structure in the longitudinal distribution of meridional wind. The longitudinal distribution of zonal wind, temperature and total ozone column is consistent with that of meridional wind and geopotential height, i.e. the middle stratosphere as a whole displays a significant longitudinal distribution at higher middle latitudes. Our results illustrate limitations of the approach via zonal mean values when studying the northern midlatitude middle stratosphere (i.e. the zonal mean of meridional component in middle latitudes masks the two-core structure and probably the significant trend).

The trends of meridional wind are found to be significant in the two core sectors independently of SSW or QBO. They are predominantly much weaker and insignificant in sectors not containing the two cores. In the period of ozone depletion deepening (1970–1995), the meridional wind in the cores intensifies, whereas in the period of recovering ozone concentration (1996–2012) it weakens. There is no pronounced dependence of these trends on the occurrence of sudden stratospheric warming and the phase of QBO. However, there is an indirect dependence of wind on QBO, as the influence of solar cycle can be seen mainly for the west phase of QBO.

Future investigations should be focused on altitudinal and seasonal extent of the two-core structure in meridional wind and related long-term trends.

Acknowledgements. The authors acknowledge support from the Grant Agency of the Czech Republic (grants P209/10/1792 and 15-03909S), from the Ministry of Education, Youth and Sports of the Czech Republic (grant LD 12070), and from the COST ES1005 project (TOSCA).

Edited by: F. Khosrawi

References

- Baldwin, M. P. and Dunkerton, T. J.: Propagation of the arctic oscillation from the stratosphere to the troposphere, *J. Geophys. Res.*, 104, 30937–30946, 1999.
- Baldwin, M. P., Shuckburgh, D., Norton, E., Thompson, W., and Gillett, G.: Weather from the Stratosphere?, *Science*, 301, 317–318, 2003.
- Bari, D., Gabriel, A., Körnich, H., and Peters, D. W. H.: The effect of zonal asymmetries in the Brewer-Dobson circulation on ozone and water vapor distributions in the northern middle atmosphere, *J. Geophys. Res. Atmos.*, 118, 3447–3466, doi:10.1029/2012JD017709, 2013.
- Baron, P., Murtagh, D. P., Urban, J., Sagawa, H., Ochiai, S., Kasai, Y., Kikuchi, K., Khosrawi, F., Körnich, H., Mizobuchi, S., Sagi, K., and Yasui, M.: Observation of horizontal winds in the middle-atmosphere between 30° S and 55° N during the northern winter 2009–2010, *Atmos. Chem. Phys.*, 13, 6049–6064, doi:10.5194/acp-13-6049-2013, 2013.
- Butchart, N.: The Brewer-Dobson circulation, *Rev. Geophys.*, 52, 157–184, doi:10.1002/2013RG000448, 2014.
- Deckert, R. and Dameris, M.: Higher tropical SSTs strengthen the tropical upwelling via deep convection, *Geophys. Res. Lett.*, 35, L10813, doi:10.1029/2008GL033719, 2008.
- Dee, D. P., Uppala, S. M., Simmons, A. J., Berrisford, P., Poli, P., Kobayashi, S., Andrae, U., Balmaseda, M. A., Balsamo, G., Bauer, P., Bechtold, P., Beljaars, A. C. M., van de Berg, L., Bidlot, J., Bormann, N., Delsol, C., Dragani, R., Fuentes, M., Geer, A. J., Haimberger, L., Healy, S. B., Hersbach, H., Hólm, E. V., Isaksen, I., Kållberg, P., Köhler, M., Matricardi, M., McNally, A. P., Monge-Sanz, B. M., Morcrette, J.-J., Park, B.-K., Peubey, C., de Rosnay, P., Tavolato, C., Thépaut, J.-N., and Vitart, F.: The ERA-Interim reanalysis: configuration and performance of the data assimilation system, *Q. J. Roy. Meteorol. Soc.*, 137, 553–597, 2011.
- Engel, A., Möbius, T., Bönisch, H., Schmidt, U., Heinz, R., Levin, I., Atlas, E., Aoki, S., Nakazawa, T., Sugawara, S., Moore, F., Hurst, D., Elkins, J., Schauffler, S., Andrews, A., and Boering, K.: Age of stratospheric air unchanged within uncertainties over the past 30 yr, *Nat. Geosci.*, 2, 28–31, doi:10.1038/ngeo388, 2009.
- Gray, L. J., Beer, J., Geller, M., Haigh, J. D., Lockwood, M., Matthes, K., Cubasch, U., Fleitmann, D., Harrison, G., Hood, L., Luterbacher, J., Meehl, G.A., Shindell, D., van Geel, B., and White, W.: Solar influences on climate, *Rev. Geophys.*, 48, RG4001, doi:10.1029/2009RG000282, 2010.
- Harris, N. R. P., Kyrö, E., Staehelin, J., Brunner, D., Andersen, S.-B., Godin-Beekmann, S., Dhomse, S., Hadjinicolaou, P., Hansen, G., Isaksen, I., Jrrar, A., Karpetchko, A., Kivi, R., Knudsen, B., Krizan, P., Lastovicka, J., Maeder, J., Orsolini, Y., Pyle, J.

- A., Rex, M., Vanicek, K., Weber, M., Wohltmann, I., Zanis, P., and Zerefos, C.: Ozone trends at northern mid- and high latitudes – A European perspective, *Ann. Geophys.*, 26, 1207–1220, doi:10.5194/angeo-26-1207-2008, 2008.
- Hartmann, D. L., Wallace, J. M., Limpasuvan, V., Thompson, D. W., and Holton, J. R.: Can ozone depletion and global warming interact to produce rapid climate change?, *P. Natl. Acad. Sci.*, 97, 1412–1417, 2000.
- Hildebrand, J., Baumgarten, G., Fiedler, J., Hoppe, U.-P., Kaifler, B., Lübken, F.-J., and Williams, B. P.: Combined wind measurements by two different lidar instruments in the Arctic middle atmosphere, *Atmos. Meas. Tech.*, 5, 2433–2445, doi:10.5194/amt-5-2433-2012, 2012.
- Holton, J. R. and Alexander, M. J.: The role of waves in transport circulation of the middle atmosphere, *Geophys. Monogr. Ser.*, 123, AGU, Washington DC, 21–35, 2000.
- Kistler, R., Collins, W., Kalnay, E., Saha, S., White, G., Woollen, J., Chelliah, M., Ebisuzaki, W., Kanamitsu, M., Kousky, V., van den Dool, H., Jenne, R., and Fiorino, M.: The NCEP 50-year reanalysis: Monthly means CDrom and documentation, *Bull. Am. Meteorol. Soc.*, 82, 247–267, 2001.
- Kodera, K., Yamazaki, K., Chiba, M., and Shibata, K.: Downward propagation of upper stratospheric mean zonal wind perturbation to the troposphere, *Geophys. Res. Lett.*, 17, 1263–1266, doi:10.1029/GL017i009p01263, 1990.
- Kozubek, M., Laštovička, J., and Křižan, P.: Differences in mid-latitude stratospheric winds between reanalysis data and versus radiosonde observations at Prague, *Ann. Geophys.*, 32, 353–366, doi:10.5194/angeo-32-353-2014, 2014.
- Labitzke, K. and Kunze, M.: Variability in the stratosphere: The Sun and the QBO, in: *Climate and Weather of the Sun-Earth System (CAWSES): Selected Papers from the Kyoto Symposium*, edited by: Tsuda, K. S. T., Fujii, R., and Geller, M., 257–278, TERRA-PUB, Tokyo, 2009.
- Labitzke, K. and van Loon, H.: Associations between the 11-year solar cycle, the QBO and the atmosphere: Part I. The troposphere and stratosphere in the Northern Hemisphere winter, *J. Atmos. Terr. Phys.*, 50, 197–206, 1988.
- Lastovicka, J., Solomon, S. C., and Qian, L.: Trends in the Neutral and Ionized Upper Atmosphere, *Space Sci. Rev.*, 168, 113–145, doi:10.1007/s11214-011-9799-3, 2012.
- Lastovicka, J., Křižan, P., and Kozubek, M.: Long-term trends in the northern extratropical ozone laminae with focus on European stations, *J. Atmos. Sol.-Terr. Phys.*, 120, 88–95, doi:10.1016/j.jastp.2014.09.006, 2014.
- Limpasuvan, V., Thompson, D. W., and Hartmann, D. L.: The life cycle of the Northern Hemisphere sudden stratospheric warmings, *J. Clim.*, 17, 2584–2596, 2004.
- Lin, P. and Fu, Q.: Changes in various branches of the Brewer-Dobson circulation from an ensemble of chemistry climate models, *J. Geophys. Res.-Atmos.*, 118, 73–84, doi:10.1029/2012JD018813, 2013.
- Manney, G. L., Santee, M. L., Rex, M., Livesey, N. J., Pitts, M. C., Veefkind, P., Nash, E. R., Wohltmann, I., Lehmann, R., Froidevaux, L., Poole, L. R., Schoeberl, M. R., Haffner, D. P., Davies, J., Dorokhov, V., Gernandt, H., Johnson, B., Kivi, R., Kyrö, E., Larsen, N., Levelt, P. F., Makshtas, A., McElroy, C. T., Nakajima, H., Parrondo, M. C., Tarasick, D. W., von der Gathen, P., Walker, K. A., and Zinoviev, N. S.: Unprecedented Arctic loss in 2011, *Nature*, 478, 469–475, doi:10.1038/nature10556, 2011.
- Marshall, A. G. and Scaife, A. A.: Impact of the QBO on surface winter climate, *J. Geophys. Res.-Atmos.*, 114, D18110, doi:10.1029/2009JD011737, 2009.
- Matsuno, T.: Vertical propagation of stationary planetary waves in the winter Northern Hemisphere, *J. Atmos. Sci.*, 27, 871–883, 1970.
- Miller, A., Schmidt, H., and Bunzel, F.: Vertical coupling of the middle atmosphere during stratospheric warming events, *J. Atmos. Sol.-Terr. Phys.*, 97, 11–21, doi:10.1016/j.jastp.2013.02.008, 2013.
- Milch, P.: Total ozone response to major geomagnetic storms during non-winter periods, *Studia Geoph. Geod.*, 38, 423–429, 1994.
- Monier, E. and Weare, B. C.: Climatology and trends in the forcing of the stratospheric ozone transport, *Atmos. Chem. Phys.*, 11, 6311–6323, doi:10.5194/acp-11-6311-2011, 2011a.
- Monier, E. and Weare, B. C.: Climatology and trends in the forcing of the stratospheric zonal-mean flow, *Atmos. Chem. Phys.*, 11, 12751–12771, doi:10.5194/acp-11-12751-2011, 2011b.
- Naito, Y. and Hirota, I.: Interannual variability of the northern winter stratospheric circulation related to the QBO and the solar cycle, *J. Meteorol. Soc. Jpn.*, 75, 925–937, 1997.
- Oberländer, S., Langematz, U., and Meul, S.: Unravelling impact factors for future changes in the Brewer-Dobson circulation, *J. Geophys. Res.-Atmos.*, 118, 10296–10312, doi:10.1002/jgrd.50775, 2013.
- Oman, L., Waugh, D. W., Pawson, S., Stolarski, R. S., and Newman, P. A.: On the influence of anthropogenic forcings on changes in the stratospheric mean age, *J. Geophys. Res.-Atmos.*, 114, D03105, doi:10.1029/2008JD010378, 2009.
- Ortland, D. A., Skinner, W. R., Hays, P. B., Burrage, M. D., Lieberman, R. S., Marshall, A. R., and Gell, D. A.: Measurements of stratospheric winds by the High Resolution Doppler Imager, *J. Geophys. Res.*, 101, 10351–10363, 1996.
- Pommereau, J.-P., Goutail, F., Lefèvre, F., Pazmino, A., Adams, C., Dorokhov, V., Eriksen, P., Kivi, R., Stebel, K., Zhao, X., and van Roozendaal, M.: Why unprecedented ozone loss in the Arctic in 2011? Is it related to climate change?, *Atmos. Chem. Phys.*, 13, 5299–5308, doi:10.5194/acp-13-5299-2013, 2013.
- Ray, E. A., Moore, F. L., Rosenlof, K. H., Davis, S. M., Sweeney, C., Tans, P., Wang, T., Elkins, J. W., Bönisch, H., Engel, A., Sugawara, S., Nakazawa, T., and Aoki, S.: Improving stratospheric transport trend analysis based on SF₆ and CO₂ measurements, *J. Geophys. Res.-Atmos.*, 119, 14–110, doi:10.1002/2014JD021802, 2014.
- Rüfenacht, R., Kämpfer, N., and Murk, A.: First middle-atmospheric zonal wind profile measurements with a new ground-based microwave Doppler-spectro-radiometer, *Atmos. Meas. Tech.*, 5, 2647–2659, doi:10.5194/amt-5-2647-2012, 2012.
- Salby, M. and Callahan, P.: Connection between the Solar Cycle and the QBO: The missing link, *J. Clim.*, 13, 2652–2662, 2000.
- Scaife, A. A., Spanghel, T., Fereday, D. R., Cubasch, U., Langematz, U., Akiyoshi, H., Slimane, B., Breasicke, P., Butchard, N., Chipperfield, M. P., Gettelman, A., Hardiman, S. C., Michou, M., Rozanov, E. and Shepherd, T. G.: Climate change projections and stratosphere-troposphere interaction, *Clim. Dynamics*, 38, 2089–2097, 2012.

- Shepherd, T. G.: Transport in the middle atmosphere, *J. Meteorol. Soc. Jpn.* II, 85B, 165–191, 2007.
- Shepherd, T. G.: Dynamics, stratospheric ozone, and climate change, *Atmos. Ocean*, 46, 117–138, 2008.
- Shindell, D., Rind, D., Balachandran, N., Lean, J., and Lonergan, P.: Solar cycle variability, ozone, and climate, *Science*, 284, 305–308, 1999.
- Sigmond, M., Scinocca, J. F., and Kushner, P. J.: Impact of the stratosphere on the tropospheric climate change, *Science*, 301, 317–318, 2008.
- Stiller, G. P., von Clarmann, T., Haedel, F., Funke, B., Glatthor, N., Grabowski, U., Kellmann, S., Kiefer, M., Linden, A., Losow, S., and López-Puertas, M.: Observed temporal evolution of global mean age of stratospheric air for the 2002 to 2010 period, *Atmos. Chem. Phys.*, 12, 3311–3331, doi:10.5194/acp-12-3311-2012, 2012.
- Wang, L. and Chen, W.: Downward arctic oscillation signal associated with moderate weak stratospheric polar vortex and the cold December 2009, *Geophys. Res. Lett.*, 37, L09707, doi:10.1029/2010GL042659, 2010.
- Waugh, D. W. and Hall, T. M.: Age of stratospheric air: Theory, observations and models, *Rev. Geophys.*, 40, 1010, doi:10.1029/2000RG000101, 2002.
- Weare, B. C.: Tropospheric-stratospheric wave propagation during El Niño-Southern Oscillation, *J. Geophys. Res.*, 115, D18122, doi:10.1029/2009JD013647, 2010.